Tensor-Based Morphometry as a Neuroimaging Biomarker for Alzheimer's Disease: An MRI Study of 676 AD, MCI, and Normal Subjects

Xue Hua[1], **Alex D. Leow, MD PhD**[1], **Neelroop Parikshak**[1], **Suh Lee**[1], **Ming-Chang Chiang, MD PhD**[1], **Arthur W. Toga, PhD**[1], **Clifford R. Jack Jr, MD**[2], **Michael W. Weiner, MD**[3,4,5], and **Paul M. Thompson, PhD**[1,*] on behalf of the Alzheimer's Disease Neuroimaging Initiative

[1]Laboratory of Neuro Imaging, Dept. of Neurology, UCLA School of Medicine, Los Angeles, CA

[2]Mayo Clinic College of Medicine, Rochester, MN

[3]Dept. Radiology, UC San Francisco, San Francisco, CA

[4]Dept. Medicine and Psychiatry, UC San Francisco, San Francisco, CA

[5]Department of Veterans Affairs Medical Center, San Francisco, CA

Abstract

In one of the largest brain MRI studies to date, we used tensor-based morphometry (TBM) to create 3D maps of structural atrophy in 676 subjects with Alzheimer's disease (AD), mild cognitive impairment (MCI), and healthy elderly controls, scanned as part of the Alzheimer's Disease Neuroimaging Initiative (ADNI). Using inverse-consistent 3D non-linear elastic image registration, we warped 676 individual brain MRI volumes to a population mean geometric template. Jacobian determinant maps were created, revealing the 3D profile of local volumetric expansion and compression. We compared the anatomical distribution of atrophy in 165 AD patients (age: 75.6 ± 7.6 years), 330 MCI subjects (74.8 ± 7.5), and 181 controls (75.9 ± 5.1). Brain atrophy in selected regions-of-interest was correlated with clinical measurements - the sum-

of-boxes clinical dementia rating (CDR-SB), mini-mental state examination (MMSE), and the logical memory test scores - at voxel level followed by correction for multiple comparisons. Baseline temporal lobe atrophy correlated with current cognitive performance, future cognitive decline, and conversion from MCI to AD over the following year; it predicted future decline even in healthy subjects. Over half of the AD and MCI subjects carried the ApoE4 (apolipoprotein E4) gene, which increases risk for AD; they showed greater hippocampal and temporal lobe deficits than non-carriers. ApoE2 gene carriers - 1/6 of the normal group - showed reduced ventricular expansion, suggesting a protective effect. As an automated image analysis technique, TBM reveals 3D correlations between neuroimaging markers, genes, and future clinical changes, and is highly efficient for large-scale MRI studies.

Introduction

Alzheimer's disease (AD) is the most common form of dementia, affecting more than 5 million individuals in the U.S. alone, and over 24 million people worldwide. Although the exact time course is unknown, AD-related pathogenesis is believed to begin decades before clinical symptoms, such as memory impairment, can be detected (Price and Morris, 1999; Goldman et al., 2001; DeKosky and Marek, 2003). Several therapeutic trials now aim to resist disease progression in those with amnestic mild cognitive impairment (MCI) – usually a transitional state between normal aging and AD - in which 10–25% of subjects develop AD within one year (Petersen et al., 1999; Petersen, 2000; Petersen et al., 2001). As AD develops, patients suffer from progressive decline in executive function, language, affect, and other cognitive and behavioral domains. To identify factors that accelerate or resist disease progression, such as treatment, genetic factors, and their interactions, it is imperative to develop biomarkers, or quantitative imaging measures, that can (1) detect abnormal aging before neuronal loss is widespread; (2) gauge the level of structural brain degeneration in way that correlates with standard cognitive measures, and (3) predict future clinical decline, or imminent conversion from MCI to AD (Mueller et al., 2005b).

Magnetic resonance imaging (MRI) is widely used in AD studies as it can non-invasively quantify gray and white matter integrity with high reproducibility (Leow et al., 2006). MRI-based measures of cortical and hippocampal atrophy have been used in recent clinical trials (Grundman et al., 2002; Jack et al., 2003), and they have been shown to correlate with pathologically confirmed neuronal loss and with the molecular hallmarks of AD (Jack et al., 2002; Silbert et al., 2003). There is interest in which MRI-based measures can optimally predict future clinical decline, often defined as conversion to AD over a specific follow-up interval (Jack et al., 1998; Scahill et al., 2003; Apostolova et al., 2006; Fleisher et al., 2008), and which measures link best with standard cognitive assessments (Fox et al., 1999; Jack et al., 2004; Thompson and Apostolova, 2007; Ridha et al., 2008).

Statistical mapping methods have also been developed to quantify brain atrophy in 3D throughout the brain, offering a detailed perspective on the anatomical distribution of disease-related changes. Tensor-based morphometry (TBM) is one such image analysis technique that identifies regional structural differences from the gradients of the nonlinear deformation fields that align, or 'warp', images to a common anatomical template (reviewed in (Ashburner and Friston, 2003)). At each voxel, a color-coded Jacobian determinant value indicates local volume excess or deficit relative to the corresponding anatomical structures in the template (Freeborough and Fox, 1998; Chung et al., 2001; Fox et al., 2001; Ashburner and Friston, 2003; Riddle et al., 2004). TBM provides a wide range of regional assessments from the voxel level to whole-brain analysis, and substructure volumes can be estimated simply by integrating Jacobian determinant values over a candidate region of interest. Since

TBM requires little manual interaction, it has been recognized as a favorable technique for very large-scale brain MRI studies and as a candidate for use in clinical trials.

In this study, we related MRI-derived TBM measurements to genetic, clinical and cognitive assessments made at the time of the scan and over the following year. We examined a large sample (N=676) to investigate genetic influences on the level of atrophy, and clinical correlations. Specifically, we were interested in correlating baseline temporal lobe atrophy, at the voxel level, with the sum-of-boxes clinical dementia rating (CDR-SB), change in CDR-SB over the following year, mini-mental state examination (MMSE), change in MMSE in the following year, the logical memory test (immediate and delayed), and conversion from MCI to AD. The goal was to determine specific regions in which atrophy predicts future decline. We also assessed ApoE gene effects on the level of atrophy, including not only the detrimental effect of the ApoE4 gene (Burggren et al., 2008; Chou et al., 2008a; Chou et al., 2008b), but also the hypothesized protective effects of the ApoE2 gene, which has been difficult to detect in small samples as its allelic frequency is relatively rare.

Materials and methods

Subjects

Imaging data was analyzed from subjects scanned as part of the Alzheimer's Disease Neuroimaging Initiative (ADNI), a large five-year study launched in 2004 by the National Institute on Aging (NIA), the National Institute of Biomedical Imaging and Bioengineering (NIBIB), the Food and Drug Administration (FDA), private pharmaceutical companies and non-profit organizations, as a $60 million, 5-year public-private partnership. The primary goal of ADNI has been to test whether serial MRI, PET, other biological markers, and clinical and neuropsychological assessments acquired in a multi-site manner mirroring enrollment methods used in clinical trials, can replicate results from smaller single site studies measuring the progression of MCI and early AD. Determination of sensitive and specific markers of very early AD progression is intended to aid researchers and clinicians to develop new treatments and monitor their effectiveness, as well as lessen the time and cost of clinical trials. The Principal Investigator of this initiative is Michael W. Weiner, M.D., VA Medical Center and University of California, San Francisco.

676 baseline MRI scans, including 165 AD patients (age: 75.6 ± 7.6 years), 330 amnsetic MCI subjects (74.8 ± 7.5 years), and 181 healthy elderly controls (75.9 ± 5.1 years), were included in this study. All subjects underwent thorough clinical and cognitive assessment at the time of scan acquisition; scores are summarized in Table 1 (in the Results section). As part of each subject's cognitive evaluation, the clinical dementia rating (CDR) was used to measure dementia severity by evaluating patients' performance in six domains: memory, orientation, judgment and problem solving, community affairs, home and hobbies, and personal care (Hughes et al., 1982; Berg, 1988; Morris, 1993). We used the 'sum-of-boxes' CDR scores (CDR-SB), which have a dynamic range of 0–18; higher scores signify poorer cognitive function. The mini-mental state examination (MMSE) was administered to provide a global measure of mental status, evaluating five cognitive domains: orientation, registration, attention and calculation, recall, and language (Folstein et al., 1975; Cockrell and Folstein, 1988). The maximum MMSE score is 30; scores of 24 or lower are generally consistent with dementia. The logical memory (LM) test is a modified version of the episodic memory assessment from the Wechsler Memory Scale-Revised (WMS-R) (Wechsler, 1987). Subjects were asked to recall a short story that consists of 25 pieces of information, both immediately after it was read to the subject, and after a 30 minute delay. A maximum score is 25 with every recalled item of information accounting for 1 point. Approximately one year after baseline, subjects returned for a follow-up brain MRI scan and

clinical assessment. Any changes in diagnosis were also noted. All AD patients met NINCDS/ADRDA criteria for probable AD (McKhann et al., 1984). ApoE genotyping was determined using DNA obtained from subjects' blood samples and was performed at the University of Pennsylvania. Please refer to the ADNI protocol for detailed inclusion and exclusion criteria (Mueller et al., 2005a; Mueller et al., 2005b).

This dataset was downloaded by February 1, 2008, and reflects the status of the database at that point; as data collection is ongoing, we focused on analyzing all available baseline scans, together with baseline and 1-year follow-up clinical and cognitive scores, as well as information on conversion from MCI to AD over the 1-year follow-up period. The study was conducted according to the Good Clinical Practice guidelines, the Declaration of Helsinki and U.S. 21 CFR Part 50-Protection of Human Subjects, and Part 56-Institutional Review Boards. Written informed consent was obtained from all participants before protocol-specific procedures, including cognitive testing, were performed.

MRI Acquisition and Image Correction

As detailed elsewhere, all subjects were scanned with a standardized MRI protocol developed for ADNI (Leow et al., 2006; Jack et al., 2008), summarized briefly here. High-resolution structural brain MRI scans were acquired at 58 ADNI sites using 1.5 Tesla MRI scanners (ADNI also collects a smaller subset of data at 3 Tesla but it was not analyzed here to avoid the additional complications of combining data across scanner field strengths). For each subject, two T1-weighted MRI scans were collected using a sagittal 3D MP-RAGE sequence. As described in a study by Jack et al. (Jack et al., 2008) typical 1.5T acquisition parameters were repetition time (TR) of 2400 ms, minimum full TE, inversion time (TI) of 1000 ms, flip angle of 8°, 24 cm field of view, $192 \times 192 \times 166$ acquisition matrix in the x-, y-, and z-dimensions, yielding a voxel size of $1.25 \times 1.25 \times 1.2$ mm^3. In plane, zero-filled reconstruction yielded a 256×256 matrix for a reconstructed voxel size of $0.9375 \times 0.9375 \times 1.2$ mm^3. The images were calibrated with phantom-based geometric corrections to ensure consistency among scans acquired at different sites (Gunter et al., 2006).

Image corrections were applied using a processing pipeline at the Mayo Clinic, consisting of: (1) a procedure termed *GradWarp* for correction of geometric distortion due to gradient non-linearity (Jovicich et al., 2006), (2) a "B1-correction", to adjust for image intensity inhomogeneity due to B1 non-uniformity using calibration scans (Jack et al., 2008), (3) "N3" bias field correction, for reducing residual intensity inhomogeneity (Sled et al., 1998), and (4) geometrical scaling, according to a phantom scan acquired for each subject (Jack et al., 2008), to adjust for scanner- and session-specific calibration errors. In addition to the original uncorrected image files, images with all of these corrections already applied (GradWarp, B1, phantom scaling, and N3) are available to the general scientific community.

Image Pre-processing

To adjust for global differences in position and scale across subjects, individual scans were linearly registered to the International Consortium for Brain Mapping template (ICBM-53) (Mazziotta et al., 2001) using 9-parameter (9P) registration (Collins et al., 1994). Globally aligned images were resampled in an isotropic space of 220 voxels along each axis (*x, y,* and *z*) with a final voxel size of 1mm^3.

Unbiased Group Average Template - Minimal Deformation Target (MDT)

A minimal deformation target (MDT) was created for the normal group to serve as an unbiased average template image (Good et al., 2001; Kochunov et al., 2002; Joshi et al., 2004; Studholme and Cardenas, 2004; Kovacevic et al., 2005; Christensen et al., 2006;

Lorenzen et al., 2006; Leporé et al., 2008). Using 40 randomly selected normal subjects, we created a customized template that facilitates automated image registration, reduces bias, and, in some studies, may improve statistical power (Leporé et al., 2007).

The process of MDT construction was detailed previously (Hua et al., 2007; Hua et al., 2008) and is described briefly here. To construct an MDT, the first step was to create an initial affine average template, by taking a voxel-wise average of the 9P globally aligned scans after intensity normalization. In the second step, a non-linear average template was built after warping individual brain scans to the affine template. We utilized a non-linear inverse consistent elastic intensity-based registration algorithm (Leow et al., 2005a; Leow et al., 2005b) which optimizes a joint cost function based on mutual information (MI) and the elastic energy of the deformation. The deformation field was computed using a spectral method to implement the Cauchy-Navier elasticity operator (Marsden and Hughes, 1983; Thompson et al., 2000b) using a Fast Fourier Transform (FFT) resolution of 32×32×32. This corresponds to an effective voxel size of 6.875 mm in the x, y, and z dimensions (220 mm / 32 = 6.875 mm). A non-linear average intensity template was then derived from the mean of the 40 deformed scans that had been non-linearly registered toward the affine average template. In a final step, the MDT was generated for the normal group by applying inverse geometric centering of the displacement fields to the non-linear average (Kochunov et al., 2002; Kochunov et al., 2005; Leporé et al., 2008).

Three-dimensional Jacobian Maps

To quantify 3D patterns of volumetric tissue change, all individual brain images (*N*=676) were non-linearly aligned to the MDT for the normal group (Leow et al., 2005a). For each subject, a separate Jacobian matrix field was derived from the gradients of the deformation field that aligned that individual brain to the MDT template. The determinant of the local Jacobian matrix was derived from the forward deformation field to characterize local volume differences. Color-coded Jacobian determinants were used to illustrate regions of volume expansion, i.e. those with det $J(r) > 1$, or contraction, i.e., det $J(r) < 1$ (Freeborough and Fox, 1998; Toga, 1999; Thompson et al., 2000a; Chung et al., 2001; Ashburner and Friston, 2003; Riddle et al., 2004) relative to the normal group template. As all images were registered to the same template, these Jacobian maps share a common anatomical coordinate defined by the normal template. Individual Jacobian maps were retained for further statistical analyses.

Pair-wise group comparisons

Using TBM, we created 676 Jacobian maps that represent individual deviations from the normal brain template. To illustrate systematic changes between groups, we constructed voxel-wise statistical maps based on a *Z* statistic (this was used instead of a Student's *t* statistic, as the number of degrees of freedom was extremely high). We computed the overall significance of group differences using permutation tests, corrected for multiple comparisons (Bullmore et al., 1999; Nichols and Holmes, 2002; Thompson et al., 2003; Chiang et al., 2007a; Chiang et al., 2007b). In brief, a null distribution for the group differences in Jacobian at each voxel was constructed using 10,000 random permutations. For each test, the subjects' diagnosis was randomly permuted and voxel-wise *Z* tests were conducted to identify voxels more significant than $p = 0.01$. The volume of voxels in the brain more significant than $p = 0.01$ was computed for the real experiment and for the random assignments. A ratio, describing the fraction of the time the suprathreshold volume was greater in the randomized maps than the real effect (the original labeling), was calculated to give an overall *P*-value for the significance of the map. This procedure has been used in many prior reports (Chiang et al., 2007a; Hua et al., 2007; Hua et al., 2008).

Regions of interest (ROIs)

The MDT template was manually parcellated using the Brainsuite software program (Shattuck and Leahy, 2002) by a trained anatomist to generate binary masks for frontal, parietal, temporal, and occipital lobes. The hippocampus was delineated on the control average template by investigators at the University College London using the MIDAS (Medical Image Display and Analysis System) software (Freeborough et al., 1997). The delineation included hippocampus proper, dentate gyrus, subiculum, and alveus (Fox et al., 1996; Scahill et al., 2003).

Correlations of Structural Brain Differences (Jacobian Values) with Clinical Measurements

At each voxel, correlations were assessed, using the general linear model, between the Jacobian values and several clinical measures – the CDR-SB, change in CDR-SB over the following year, MMSE, change of MMSE over the following year, logical memory test (immediate and delayed), and conversion from MCI to AD during the following year. As Jacobian maps are composed of signals denoting both CSF expansion (J>1) and tissue loss (J<1), we performed separate evaluations of the positive, negative and two-sided associations. The results of voxel-wise correlations were corrected for multiple comparisons by permutation testing. In each random sample, clinical scores were randomly assigned to each subject and the number of voxels with significant correlations ($p \leq 0.01$) was recorded. After 10,000 permutations, a ratio was calculated describing the fraction of the null simulations in which a statistical effect had occurred with similar or greater magnitude than the real effects. This ratio served as an estimate of the overall significance of the correlations, corrected for multiple comparisons, as performed in many prior studies (Nichols and Holmes, 2002). The number of permutations N was chosen to be 10,000, to control the standard error SEp of the omnibus probability p, which follows a binomial distribution $B(N, p)$ with known standard error (Edgington, 1995). When $N = 10,000$, the approximate margin of error (95% confidence interval) for p is around 5% of p.

Influence of Genetic Variants on Brain Structures

To investigate how apolipoprotein E (ApoE) genotype modulates brain structure in each diagnostic group, we created age- and gender-matched groups for each diagnosis, categorized by their different combinations of ApoE alleles. Carriers of an ApoE2 gene (which confers lower risk for AD than that of the general population) or an ApoE4 gene (which increases risk for developing AD relative to that of the general population) were compared with homozygous ApoE3, which is the commonest genotype (Corder et al., 1993; Saunders et al., 1993; Roses and Saunders, 1994). Group differences were quantified using voxel-wise *Z*-tests followed by permutations to correct for multiple comparisons, as described earlier.

Results

3D Profiles of Brain Atrophy

We conducted pair-wise comparisons among AD ($N = 165$), MCI ($N = 330$) and normal ($N = 181$) groups. From individual Jacobian maps, we derived mean group difference maps and statistical maps based on the *Z* test. The 3D map comparing AD with normal controls revealed profound atrophy of the hippocampus and temporal lobes bilaterally in AD, accompanied by CSF expansion in the lateral ventricles and circular sulcus of the *insula* (Figure 1a). The MCI group displayed similar patterns of atrophy as AD but to a much lesser extent, with more anatomically restricted temporal lobe deficits (Figure 1b). Additional temporal lobe atrophy was apparent when contrasting the AD and MCI groups (Figure 1c). Permutation tests confirmed significant group differences in all three pair-wise comparisons

using a whole-brain ROI, corrected for multiple comparisons. The two-tailed corrected P values were: $P < 0.001$ for AD vs. Normal, $P < 0.001$ for MCI vs. Normal, and $P = 0.003$ for AD vs. MCI.

Correlations with Clinical Measurements

There is great interest in determining regions of the brain in which atrophy is most strongly correlated with established measures of cognitive or clinical decline, or with future outcome measures, such as imminent conversion to AD. These measures could potentially be used to inform prognosis or monitor drug treatment efficacy. Results from the temporal lobe ROI are shown below.

Sum-of-boxes CDR and future cognitive decline

In both AD and MCI groups, the levels of baseline temporal lobe atrophy were correlated with the sum-of-boxes CDR scores. The negative correlations in Figure 2a identify regions in which tissue loss was linked with higher CDR-SB scores, i.e., more impaired cognitive function. The significance is slightly greater for the MCI than the AD group, perhaps partly due to the greater sample size for the MCI group. This test was not significant within the normal group, due to the low variance in CDR-SB scores. Additionally, we examined the correlation between the Jacobian values (which reflect structure volumes at baseline) and the changes in CDR-SB over the following year (Figure 2b). In all three groups, independently, there was a significant negative correlation, suggesting that baseline temporal atrophy predicts future cognitive decline.

MMSE and future cognitive decline

In the MCI group, we found a significant positive correlation between *baseline* temporal atrophy and MMSE scores (Figure 3a); note that lower MMSE scores designate greater cognitive impairment. However, we did not detect such a correlation either in the AD or in the normal group. The control group showed very little variation in the MMSE scores, so a correlation was not expected. Although a correlation was expected in the AD group, it may not have been detected due to the smaller sample size. In the AD group however, lower Jacobian values (or more tissue loss) were linked to a *future decline* in MMSE scores over the following 1-year follow-up interval (Figure 3b). This is consistent with the intriguing hypothesis that atrophic change may accelerate in AD, so that individuals with greater level of atrophy also show greater rates of decline in the immediate future. This correlation with future decline was not detected as significant for the MCI and normal groups, perhaps because they had more limited changes in cognition measured by MMSE scores (MMSE changes for all 3 groups are shown in Figure 3b).

Wechsler memory scale-revised (WMS-R) logical memory, immediate and delayed recall

In all three groups, independently, there was a significant positive correlation between the level of atrophy and logical memory test scores for both immediate (Figure 4a) and delayed (Figure 4b) conditions. This finding suggests that temporal lobe degeneration is coupled with diminishing episodic memory performance. Intriguingly, the hippocampus and entorhinal cortex were not the areas most strongly correlated with impaired memory performance. This may be due to the slightly lower sensitivity of TBM for detecting changes in very small structures. Many AD and MCI subjects perform very poorly on this memory test, thus restricting the range and perhaps accounting for the highest correlation being found in the controls.

Future Conversion from MCI to AD

The subjects who returned for 1-year follow-up were evaluated for any change in clinical diagnosis. Of the 186 MCI subjects followed from baseline, who had been assessed at the time of writing this report, 40 individuals had developed AD after 1 year, corresponding to a conversion rate of 21.5%. This rate is slightly higher than that typically found in prior studies, which report an annual conversion rate from MCI to AD of around 12% (ranging from 6% to 25% per year) (Petersen et al., 1999; Petersen et al., 2001). Figure 5 suggests that patients with greater temporal lobe atrophy are more prone to develop AD in the future. The corrected *P* value is 0.02, so this association is significant overall, after correction for multiple comparisons.

ApoE Genetic Influence

There is great interest in whether common variants of the ApoE gene influence brain structure, as they are known to affect the future risk of developing AD. Table 2 summarizes the genotype frequencies in the subset of the ADNI sample examined in this report. In the AD group, approximately 67% of the subjects carried one or two copies of the ApoE4 gene (each copy confers increased risk for AD). There was a trend for a slightly higher incidence of ApoE4 in men than in women (*p*=0.07; *chi-squared test*). The frequency of ApoE4 was around 52% in the MCI group, and only 26% in the normal group. In contrast, carriers of the ApoE2 gene (with genotypes ε2/ε2 and ε2/ε3) were mainly found in the normal group. Around 17% of normal subjects carried a copy of the ε2 allele, most of whom are ε2/ε3 (ε2/ε2 and ε2/ε4 are rare, occurring in only ~1% of normal subjects, and they were not included in our comparisons of genetic groups; Table 2). In other words, we only compared E2/3 with E3/3, rather than lump E2/4, E2/2 and E2/3 together. This distinction was made because it is especially hard to interpret the effect of E2 if E2/4 subjects are lumped together with E2/3 and E2/2 subjects.

We found that, in healthy subjects, the presence of ApoE2 was associated with reduced CSF volume in the ventricular system (Figure 6a), when compared with homozygous ApoE3 carriers. This may support the hypothesis that this genotype has a protective effect. ApoE4 showed a dose-dependent detrimental effect. One copy of ApoE4 was associated with increased CSF expansion in the Sylvian fissures, between superior temporal and inferior frontal lobes (Figure 6b). This could be an early indicator of temporal lobe atrophy. Next we compared the ApoE4 homozygotes (ε4/ε4) with the heterozygotes (ε3/ε4), in the MCI and AD groups. Even within these groups, greater hippocampal (Figure 6c) and temporal lobe (Figure 6d) atrophy was associated with carrying an additional ApoE4 allele.

Discussion

In one of the largest TBM studies to date, and one of the largest MRI studies of AD and MCI, we found that baseline temporal lobe atrophy (1) correlates with cognitive impairment (measured using CDR-SB, MMSE, and logical memory test scores), (2) predicts future cognitive decline (in terms of the CDR-SB), in all of the AD, MCI, and normal groups, and (3) predicts conversion from MCI to AD, over a subsequent one-year period. We found a dose-dependent association of the ApoE4 gene with greater structural atrophy, and for the first time, we established neuroimaging evidence for a protective effect of the ApoE2 gene in healthy controls. ApoE2 carriers – who made up around 1/6 of the normal group - showed more limited ventricular expansion, which likely reflects preservation of brain parenchyma.

In an initial pilot study (*N = 120*) (Hua et al., 2008), our main aim was to determine which types of parameter selections in TBM (e.g., 9- or 12-parameter global alignment, cross-subject versus group template registration) would be optimal to detect group differences

between AD and normal subjects. In such a small sample (only 40 per group), we were barely able to differentiate MCI and normal groups, and with 120 subjects in total, correlations with clinical scores were significant only when all three groups were pooled together. It is common practice to combine various diagnostic groups (e.g., AD, MCI and normal) to achieve a greater range of disease severity for correlations with MRI volumetric measurements. In the current study, we used a sample size that was almost five times greater, which allowed us to detect correlations even *within* the diagnostic categories. Not only did we detect significant differences between MCI and normal, but we were also able to correlate temporal lobe atrophy at baseline with a variety of clinical measures and cognitive test scores, independently within each diagnostic group. TBM-based computations of temporal lobe atrophy predicted future cognitive decline (annual change in CDR-SB) even in the healthy subjects. The risk of deteriorating from MCI to AD in the one year period after the baseline scan was considerably greater among those with greater temporal lobe atrophy. Our results agree with prior studies suggesting that the level of atrophy in the hippocampus, entorhinal cortex, whole brain, and the degree of lateral ventricular expansion, are typically greater in MCI converters versus stable MCI subjects (Bozzali et al., 2006; Jack et al., 2004). Given the effect sizes, our samples are close to the minimal sizes necessary to detect these effects with TBM; this information may be useful in planning future studies, including therapeutic trials.

Our finding that MCI converters have greater baseline atrophy than those who remain stable agrees with several prior reports. It has been shown that MRI can predict likelihood of (or time to) progression from MCI to AD (Jack et al., 1999). In Apostolova et al. (Apostolova et al., 2006), we found distinct patterns of hippocampal atrophy in MCI subjects who remained stable or recovered, versus those who declined, over a 3-year follow-up period. In a recent VBM study, MCI converters showed more widespread areas of reduced gray matter density than MCI non-converters, but in a similar pattern to that seen in AD (Bozzali et al., 2006).

AD pathology follows a characteristic anatomical trajectory, with the earliest observable changes in the entorhinal cortex and hippocampus, then moving to temporal and parietal lobes, and finally affecting the frontal lobes in the late stages of AD (Braak and Braak, 1991; Thompson et al., 2003; Thompson and Apostolova, 2007). With that in mind, we were interested in assessing genetic influences on structural differences in the temporal lobes and ventricular regions, as they are among the earliest to show disease-related atrophy.

The apolipoprotein E (ApoE) gene is located on chromosome 19 with three alleles (ApoE2, ApoE3, ApoE4) (Zannis and Breslow, 1982; Zannis et al., 1982). ApoE3 is the commonest allelic variant, while ApoE4 increases and ApoE2 decreases susceptibility to AD (Corder et al., 1993; Saunders et al., 1993; Corder et al., 1994; Blacker et al., 2007;). ApoE4 is over-represented in the AD population (Table 2) and confers a dose-dependent risk, in which two E4 alleles confer greater risk than one (Corder et al., 1993; Geroldi et al., 1999). ApoE4 homozygotes (ε4/ε4) typically show greater deficits than ApoE4 heterozygotes (ε3/ε4) with similar demographic risk factors (Geroldi et al., 2000; Lehtovirta et al., 2000; Martins et al., 2005).

We were able to demonstrate genetic effects on brain structure, even among healthy elderly subjects. 17% - or around one-sixth - of the normal controls carried an ApoE2 allele, and had smaller ventricular volume than homozygous ApoE3 carriers, which is the commonest genotype. As progressive ventricular enlargement is a typical process during normal aging and brain degeneration, this neuroimaging evidence may reflect a protective effect of ApoE2 on the surrounding brain parenchyma, detected as an effect on ventricular size. We also found a dose-dependent effect of ApoE4. In MCI, one copy of ApoE4 was not detectably associated with temporal lobe differences, but it was associated with elevated CSF volume

in the Sylvian fissures, a region where changes are commonly seen in the initial phase of temporal lobe degeneration. An additional copy of ApoE4 was associated with further hippocampal atrophy in MCI, and was correlated with still further deterioration of temporal lobe structures in AD. The dose-dependent effect of ApoE4 seems to mirror an accelerated AD progression in the same topography as typical AD development, starting in the entorhinal cortex and hippocampus at the MCI stage, then moving on to temporal and parietal lobes in AD.

Our ApoE4 genetic findings are consistent with prior MRI studies. Several MRI studies have shown reduced hippocampal cross-sectional area (Tohgi et al., 1997; Moffat et al., 2000) and greater volumetric atrophy in the entorhinal cortex (Juottonen et al., 1998; Geroldi et al., 1999; Jack et al., 2007) in ApoE4 carriers versus non-carriers. Using the brain boundary shift integral method, and iterative principal component analysis, accelerated whole brain atrophy was associated with ApoE4 gene in a dose-dependent way (Chen et al., 2007). Recently, voxel-based morphometry (VBM) has made it easier to map the profile of genetic influences throughout the entire brain, without restriction to pre-defined regions-of-interest. In a large VBM study of 750 healthy elderly subjects, ApoE4 homozygotes displayed significant medial temporal lobe deficits as compared to ApoE4 heterozygotes and non-carrier subjects (Lemaitre et al., 2005). In another VBM study of cognitively normal subjects, ApoE3/ApoE4 carriers, relative to non-carriers, showed regionally reduced gray matter density in right medial temporal and bilateral frontotemporal regions (Wishart et al., 2006). Although we did not find an ApoE4 effect on brain morphology in normal subjects here, we recently detected abnormal ventricular expansion in a different sample of healthy elderly ApoE4 carriers versus non-carriers, by developing a automated method to extract 3D surface-based models of the lateral ventricles (Chou et al., 2008b) As that method combined multiple fluid registrations to create increasingly accurate models of specific anatomical structures, it may be that an ApoE4 effect in normals could be detectable using a multi-atlas version of TBM (cf. Chou et al., 2008) or by using other methods that directly model the affected anatomical structures. For example, we recently applied a cortical flattening and thickness mapping approach to the entorhinal cortex, and found thinner cortex in specific hippocampal subregions in cognitively normal ApoE4 carriers versus non-carriers (Burggren et al., 2008). Lastly, another reason we may have found an ApoE4 effect in MCI but not in normals is that our MCI group was almost twice the size (N=323) of our normal group (N=179), and around half of the MCI subjects but only a quarter of the controls carried ApoE4. The power to detect an effect was therefore greater in the MCI group. In other words, our detection of ApoE4 effects in MCI but not controls does not imply the effect size is any greater in MCI. Conversely, the protective ApoE2 effect we found in controls may also be equally present in MCI or AD subjects, but the genotype is so rare in AD and MCI that sufficient numbers of ApoE2 subjects could not be found to provide adequate power. Using placebo subjects in a recent study of vitamin E and donepezil in MCI, Jack et al. (2007) found that rates of hippocampal atrophy were greater in E4 carriers than non carriers (but not significantly different between E4 homozygotes than heterozygotes – although this latter finding could just be due to small numbers).

VBM is an unbiased technique that has been applied to various MRI studies of AD, MCI and normal subjects to provide a comprehensive view of normal aging as well as brain degeneration. Good et al. (2001) used VBM to examine the effects of age on brain tissue volumes in 465 normal adults (Good et al., 2001). Global gray matter volume was shown to decrease linearly with age, with accelerated loss in the insula, superior parietal gyri, central sulci, and cingulate sulci bilaterally. In contrast, regions such as the amygdalae, hippocampi, and entorhinal cortices were relatively preserved during normal aging. Similar time-lapse trajectories were computed in our recent cortical thickness analysis of 176 subjects aged 7 to 87, with temporal lobe atrophy accelerating in normal old age (Sowell et al., 2007; Sowell et

al., 2003). Smith et al. (Smith et al., 2007) prospectively followed 136 cognitively normal elderly and 5 MCI subjects with MRI for an average of 5.4 years. 23 of them converted to MCI and 9 of the 23 further deteriorated to meet criteria for AD. At baseline, the group consisting of the 23 pre-MCI/pre-AD and the 5 MCI subjects demonstrated significant gray matter atrophy in the anteromedial temporal and left angular gyri, and the left lateral temporal lobe. VBM revealed clusters of gray matter loss in bilateral medial temporal, posterior cingulate, and temporoparietal structures in AD (Baron et al., 2001). Optimized VBM was used to demonstrate gradually reduced global gray matter volume from MCI to AD compared to normal, characterized by medial temporal lobe damage in MCI and additional parietal and cingulate cortices loss in AD (Karas et al., 2004), in a pattern that we recently confirmed using cortical mapping methods (Apostolova et al., 2007; Frisoni et al., 2008). Chetelat et al. examined 18 MCI subjects of whom 7 converted to AD during an 18-month follow-up interval (Chetelat et al., 2005). Fastest atrophy rates were identified in the temporal pole, entorhinal and lateral temporal cortices (2.5–4.5%). The prefrontal cortex was more affected in non-converters. At baseline, greater cortical involvement was seen in the parahippocampal, fusiform, lingual and posterior cingulate cortices in MCI subjects who later converted to AD versus those who did not.

TBM-based analysis is a powerful tool with potential to monitor structural atrophy in AD at the incipient stage, before severe cognitive impairment takes place. Recent developments in TBM have included a method called DARTEL, an algorithm for diffeomorphic image registration (Ashburner, 2007). It was applied to a large MRI dataset (N = 471) to automatically extract information regarding gender and age effects on brain morphometry. These studies and ours show that TBM is a highly automated technique, capable of revealing voxel-level associations between neuroimaging markers and clinical or genetic variation. TBM should facilitate the discovery of factors that influence disease progression, as well as protective factors, in large-scale MRI studies.

References

Apostolova LG, Dutton RA, Dinov ID, Hayashi KM, Toga AW, Cummings JL, Thompson PM. Conversion of mild cognitive impairment to Alzheimer disease predicted by hippocampal atrophy maps. Arch Neurol. 2006; 63:693–699. [PubMed: 16682538]

Apostolova LG, Steiner CA, Akopyan GG, Dutton RA, Hayashi KM, Toga AW, Cummings JL, Thompson PM. Three-dimensional gray matter atrophy mapping in mild cognitive impairment and mild Alzheimer disease. Arch Neurol. 2007; 64:1489–1495. [PubMed: 17923632]

Ashburner J. A fast diffeomorphic image registration algorithm. Neuroimage. 2007; 38:95–113. [PubMed: 17761438]

Ashburner, J.; Friston, KJ. Human Brain Function. Academic Press; 2003. Morphometry.

Baron JC, Chetelat G, Desgranges B, Perchey G, Landeau B, de la Sayette V, Eustache F. In vivo mapping of gray matter loss with voxel-based morphometry in mild Alzheimer's disease. Neuroimage. 2001; 14:298–309. [PubMed: 11467904]

Berg L. Clinical Dementia Rating (CDR). Psychopharmacol Bull. 1988; 24:637–639. [PubMed: 3249765]

Blacker D, Lee H, Muzikansky A, Martin EC, Tanzi R, McArdle JJ, Moss M, Albert M. Neuropsychological measures in normal individuals that predict subsequent cognitive decline. Arch Neurol. 2007; 64:862–871. [PubMed: 17562935]

Bozzali M, Filippi M, Magnani G, Cercignani M, Franceschi M, Schiatti E, Castiglioni S, Mossini R, Falautano M, Scotti G, Comi G, Falini A. The contribution of voxel-based morphometry in staging patients with mild cognitive impairment. Neurology. 2006; 67:453–460. [PubMed: 16894107]

Braak H, Braak E. Neuropathological stageing of Alzheimer-related changes. Acta Neuropathol (Berl). 1991; 82:239–259. [PubMed: 1759558]

Bullmore ET, Suckling J, Overmeyer S, Rabe-Hesketh S, Taylor E, Brammer MJ. Global, voxel, and cluster tests, by theory and permutation, for a difference between two groups of structural MR images of the brain. IEEE Trans Med Imaging. 1999; 18:32–42. [PubMed: 10193695]

Burggren AC, Zeineh MM, Ekstrom AE, Braskie M, Thompson PM, Small GW, Bookheimer S. Reduced Cortical Thickness In Hippocampal Subregions among Cognitively Normal Apolipoprotein E e4 Carriers. Neuroimage. 2008 revised version submitted, March 2008.

Carmichael OT, Kuller LH, Lopez OL, Thompson PM, Dutton RA, Lu A, Lee SE, Lee JY, Aizenstein HJ, Meltzer CC, Liu Y, Toga AW, Becker JT. Acceleration of cerebral ventricular expansion in the Cardiovascular Health Study. Neurobiol Aging. 2007a; 28:1316–1321. [PubMed: 16875759]

Carmichael OT, Kuller LH, Lopez OL, Thompson PM, Dutton RA, Lu A, Lee SE, Lee JY, Aizenstein HJ, Meltzer CC, Liu Y, Toga AW, Becker JT. Cerebral ventricular changes associated with transitions between normal cognitive function, mild cognitive impairment, and dementia. Alzheimer Dis Assoc Disord. 2007b; 21:14–24. [PubMed: 17334268]

Chen K, Reiman EM, Alexander GE, Caselli RJ, Gerkin R, Bandy D, Domb A, Osborne D, Fox N, Crum WR, Saunders AM, Hardy J. Correlations between apolipoprotein E epsilon4 gene dose and whole brain atrophy rates. Am J Psychiatry. 2007; 164:916–921. [PubMed: 17541051]

Chetelat G, Landeau B, Eustache F, Mezenge F, Viader F, de la Sayette V, Desgranges B, Baron JC. Using voxel-based morphometry to map the structural changes associated with rapid conversion in MCI: a longitudinal MRI study. Neuroimage. 2005; 27:934–946. [PubMed: 15979341]

Chiang MC, Dutton RA, Hayashi KM, Lopez OL, Aizenstein HJ, Toga AW, Becker JT, Thompson PM. 3D pattern of brain atrophy in HIV/AIDS visualized using tensor-based morphometry. Neuroimage. 2007a; 34:44–60. [PubMed: 17035049]

Chiang MC, Reiss AL, Lee AD, Bellugi U, Galaburda AM, Korenberg JR, Mills DL, Toga AW, Thompson PM. 3D pattern of brain abnormalities in Williams syndrome visualized using tensor-based morphometry. Neuroimage. 2007b; 36:1096–1109. [PubMed: 17512756]

Chou YY, Leporé N, Avedissian C, Madsen SK, Hua X, Jack CR Jr, Weiner MW, Toga AW, Thompson PM. Mapping Ventricular Expansion and its Clinical Correlates in Alzheimer's Disease and Mild Cognitive Impairment using Multi-Atlas Fluid Image Alignment. MICCAI. 2008a; 2008 submitted, March 2008.

Chou YY, Lepore N, de Zubicaray GI, Carmichael OT, Becker JT, Toga AW, Thompson PM. Automated ventricular mapping with multi-atlas fluid image alignment reveals genetic effects in Alzheimer's disease. Neuroimage. 2008b; 40:615–630. [PubMed: 18222096]

Christensen GE, Johnson HJ, Vannier MW. Synthesizing average 3D anatomical shapes. Neuroimage. 2006; 32:146–158. [PubMed: 16697223]

Chung MK, Worsley KJ, Paus T, Cherif C, Collins DL, Giedd JN, Rapoport JL, Evans AC. A unified statistical approach to deformation-based morphometry. Neuroimage. 2001; 14:595–606. [PubMed: 11506533]

Cockrell JR, Folstein MF. Mini-Mental State Examination (MMSE). Psychopharmacol Bull. 1988; 24:689–692. [PubMed: 3249771]

Collins DL, Neelin P, Peters TM, Evans AC. Automatic 3D intersubject registration of MR volumetric data in standardized Talairach space. J Comput Assist Tomogr. 1994; 18:192–205. [PubMed: 8126267]

Corder EH, Saunders AM, Risch NJ, Strittmatter WJ, Schmechel DE, Gaskell PC Jr, Rimmler JB, Locke PA, Conneally PM, Schmader KE, et al. Protective effect of apolipoprotein E type 2 allele for late onset Alzheimer disease. Nat Genet. 1994; 7:180–184. [PubMed: 7920638]

Corder EH, Saunders AM, Strittmatter WJ, Schmechel DE, Gaskell PC, Small GW, Roses AD, Haines JL, Pericak-Vance MA. Gene dose of apolipoprotein E type 4 allele and the risk of Alzheimer's disease in late onset families. Science. 1993; 261:921–923. [PubMed: 8346443]

DeKosky ST, Marek K. Looking backward to move forward: early detection of neurodegenerative disorders. Science. 2003; 302:830–834. [PubMed: 14593169]

Fleisher AS, Sun S, Taylor C, Ward CP, Gamst AC, Petersen RC, Jack CR Jr, Aisen PS, Thal LJ. Volumetric MRI vs clinical predictors of Alzheimer disease in mild cognitive impairment. Neurology. 2008; 70:191–199. [PubMed: 18195264]

Folstein MF, Folstein SE, McHugh PR. "Mini-mental state". A practical method for grading the cognitive state of patients for the clinician. J Psychiatr Res. 1975; 12:189–198. [PubMed: 1202204]

Fox NC, Crum WR, Scahill RI, Stevens JM, Janssen JC, Rossor MN. Imaging of onset and progression of Alzheimer's disease with voxel-compression mapping of serial magnetic resonance images. Lancet. 2001; 358:201–205. [PubMed: 11476837]

Fox NC, Scahill RI, Crum WR, Rossor MN. Correlation between rates of brain atrophy and cognitive decline in AD. Neurology. 1999; 52:1687–1689. [PubMed: 10331700]

Fox NC, Warrington EK, Freeborough PA, Hartikainen P, Kennedy AM, Stevens JM, Rossor MN. Presymptomatic hippocampal atrophy in Alzheimer's disease. A longitudinal MRI study. Brain. 1996; 119(Pt 6):2001–2007. [PubMed: 9010004]

Freeborough PA, Fox NC. Modeling brain deformations in Alzheimer disease by fluid registration of serial 3D MR images. J Comput Assist Tomogr. 1998; 22:838–843. [PubMed: 9754126]

Freeborough PA, Fox NC, Kitney RI. Interactive algorithms for the segmentation and quantitation of 3-D MRI brain scans. Comput Methods Programs Biomed. 1997; 53:15–25. [PubMed: 9113464]

Frisoni GB, Prestia A, Rasser PE, Bonetti M, Thompson PM. In vivo mapping of incremental cortical atrophy from health to incipient and overt Alzheimer's disease. 2008 to be submitted, March 2008.

Geroldi C, Laakso MP, DeCarli C, Beltramello A, Bianchetti A, Soininen H, Trabucchi M, Frisoni GB. Apolipoprotein E genotype and hippocampal asymmetry in Alzheimer's disease: a volumetric MRI study. J Neurol Neurosurg Psychiatry. 2000; 68:93–96. [PubMed: 10601411]

Geroldi C, Pihlajamaki M, Laakso MP, DeCarli C, Beltramello A, Bianchetti A, Soininen H, Trabucchi M, Frisoni GB. APOE-epsilon4 is associated with less frontal and more medial temporal lobe atrophy in AD. Neurology. 1999; 53:1825–1832. [PubMed: 10563634]

Goldman WP, Price JL, Storandt M, Grant EA, McKeel DW Jr, Rubin EH, Morris JC. Absence of cognitive impairment or decline in preclinical Alzheimer's disease. Neurology. 2001; 56:361–367. [PubMed: 11171902]

Good CD, Johnsrude IS, Ashburner J, Henson RN, Friston KJ, Frackowiak RS. A voxel-based morphometric study of ageing in 465 normal adult human brains. Neuroimage. 2001; 14:21–36. [PubMed: 11525331]

Grundman M, Sencakova D, Jack CR Jr, Petersen RC, Kim HT, Schultz A, Weiner MF, DeCarli C, DeKosky ST, van Dyck C, Thomas RG, Thal LJ. Brain MRI hippocampal volume and prediction of clinical status in a mild cognitive impairment trial. J Mol Neurosci. 2002; 19:23–27. [PubMed: 12212787]

Gunter, J.; Bernstein, M.; Borowski, B.; Felmlee, J.; Blezek, D.; Mallozzi, R. Validation testing of the MRI calibration phantom for the Alzheimer's Disease Neuroimaging Initiative Study; ISMRM 14th Scientific Meeting and Exhibition; 2006.

Hua X, Leow AD, Lee S, Klunder AD, Toga AW, Leporé N, Chou YY, Brun C, Chiang MC, Barysheva M, Jack CR Jr, Bernstein MA, Britson PJ, Ward CP, Whitwell JL, Borowski B, Fleisher AS, Fox NC, Boyes R, Barnes J, Harvey D, Kornak J, Schuff N, Boreta L, Alexander GE, Weiner MW, Thompson PM. 3D Characterization of Brain Atrophy in Alzheimer's Disease and Mild Cognitive Impairment using Tensor-Based Morphometry. Neuroimage. 2008

Hua X, Leow AD, Levitt JG, Caplan R, Thompson PM, Toga AW. Detecting brain growth patterns in normal children using tensor-based morphometry. Hum Brain Mapp. 2007

Hughes CP, Berg L, Danziger WL, Coben LA, Martin RL. A new clinical scale for the staging of dementia. Br J Psychiatry. 1982; 140:566–572. [PubMed: 7104545]

Jack CR Jr, Bernstein MA, Fox NC, Thompson P, Alexander G, Harvey D, Borowski B, Britson PJ, J LW, Ward C, Dale AM, Felmlee JP, Gunter JL, Hill DL, Killiany R, Schuff N, Fox-Bosetti S, Lin C, Studholme C, Decarli CS, Ward HA, Metzger GJ, Scott KT, Mallozzi R, Blezek D, Levy J, Debbins JP, Fleisher AS, Albert M, Green R, Bartzokis G, Glover G, Mugler J, Weiner MW. The Alzheimer's disease neuroimaging initiative (ADNI): MRI methods. J Magn Reson Imaging. 2008

Jack CR Jr, Dickson DW, Parisi JE, Xu YC, Cha RH, O'Brien PC, Edland SD, Smith GE, Boeve BF, Tangalos EG, Kokmen E, Petersen RC. Antemortem MRI findings correlate with hippocampal neuropathology in typical aging and dementia. Neurology. 2002; 58:750–757. [PubMed: 11889239]

Jack CR Jr, Petersen RC, Grundman M, Jin S, Gamst A, Ward CP, Sencakova D, Doody RS, Thal LJ. Longitudinal MRI findings from the vitamin E and donepezil treatment study for MCI. Neurobiol Aging. 2007

Jack CR Jr, Petersen RC, Xu Y, O'Brien PC, Smith GE, Ivnik RJ, Tangalos EG, Kokmen E. Rate of medial temporal lobe atrophy in typical aging and Alzheimer's disease. Neurology. 1998; 51:993–999. [PubMed: 9781519]

Jack CR Jr, Petersen RC, Xu YC, O'Brien PC, Smith GE, Ivnik RJ, Boeve BF, Waring SC, Tangalos EG, Kokmen E. Prediction of AD with MRI-based hippocampal volume in mild cognitive impairment. Neurology. 1999; 52:1397–1403. [PubMed: 10227624]

Jack CR Jr, Shiung MM, Gunter JL, O'Brien PC, Weigand SD, Knopman DS, Boeve BF, Ivnik RJ, Smith GE, Cha RH, Tangalos EG, Petersen RC. Comparison of different MRI brain atrophy rate measures with clinical disease progression in AD. Neurology. 2004; 62:591–600. [PubMed: 14981176]

Jack CR Jr, Slomkowski M, Gracon S, Hoover TM, Felmlee JP, Stewart K, Xu Y, Shiung M, O'Brien PC, Cha R, Knopman D, Petersen RC. MRI as a biomarker of disease progression in a therapeutic trial of milameline for AD. Neurology. 2003; 60:253–260. [PubMed: 12552040]

Joshi S, Davis B, Jomier M, Gerig G. Unbiased diffeomorphic atlas construction for computational anatomy. Neuroimage. 2004; 23 Suppl 1:S151–S160. [PubMed: 15501084]

Jovicich J, Czanner S, Greve D, Haley E, van der Kouwe A, Gollub R, Kennedy D, Schmitt F, Brown G, Macfall J, Fischl B, Dale A. Reliability in multi-site structural MRI studies: effects of gradient non-linearity correction on phantom and human data. Neuroimage. 2006; 30:436–443. [PubMed: 16300968]

Juottonen K, Lehtovirta M, Helisalmi S, Riekkinen PJ Sr, Soininen H. Major decrease in the volume of the entorhinal cortex in patients with Alzheimer's disease carrying the apolipoprotein E epsilon4 allele. J Neurol Neurosurg Psychiatry. 1998; 65:322–327. [PubMed: 9728943]

Karas GB, Scheltens P, Rombouts SA, Visser PJ, van Schijndel RA, Fox NC, Barkhof F. Global and local gray matter loss in mild cognitive impairment and Alzheimer's disease. Neuroimage. 2004; 23:708–716. [PubMed: 15488420]

Kochunov P, Lancaster J, Hardies J, Thompson PM, Woods RP, Cody JD, Hale DE, Laird A, Fox PT. Mapping structural differences of the corpus callosum in individuals with 18q deletions using targetless regional spatial normalization. Hum Brain Mapp. 2005; 24:325–331. [PubMed: 15704090]

Kochunov P, Lancaster J, Thompson P, Toga AW, Brewer P, Hardies J, Fox P. An optimized individual target brain in the Talairach coordinate system. Neuroimage. 2002; 17:922–927. [PubMed: 12377166]

Kovacevic N, Henderson JT, Chan E, Lifshitz N, Bishop J, Evans AC, Henkelman RM, Chen XJ. A three-dimensional MRI atlas of the mouse brain with estimates of the average and variability. Cereb Cortex. 2005; 15:639–645. [PubMed: 15342433]

Lehtovirta M, Laakso MP, Frisoni GB, Soininen H. How does the apolipoprotein E genotype modulate the brain in aging and in Alzheimer's disease? A review of neuroimaging studies. Neurobiol Aging. 2000; 21:293–300. [PubMed: 10867214]

Lemaitre H, Crivello F, Dufouil C, Grassiot B, Tzourio C, Alperovitch A, Mazoyer B. No epsilon4 gene dose effect on hippocampal atrophy in a large MRI database of healthy elderly subjects. Neuroimage. 2005; 24:1205–1213. [PubMed: 15670698]

Leow, A.; Huang, SC.; Geng, A.; Becker, JT.; Davis, S.; Toga, AW.; Thompson, PM. Inverse Consistent Mapping in 3D Deformable Image Registration: Its Construction and Statistical Properties. Glenwood Springs, Colorado, USA: Information Processing in Medical Imaging; 2005a. p. 493-503.

Leow AD, Klunder AD, Jack CR Jr, Toga AW, Dale AM, Bernstein MA, Britson PJ, Gunter JL, Ward CP, Whitwell JL, Borowski BJ, Fleisher AS, Fox NC, Harvey D, Kornak J, Schuff N, Studholme C, Alexander GE, Weiner MW, Thompson PM. Longitudinal stability of MRI for mapping brain change using tensor-based morphometry. Neuroimage. 2006; 31:627–640. [PubMed: 16480900]

Leow, AD.; Thompson, PM.; Hayashi, KM.; Bearden, C.; Nicoletti, MA.; Monkul, SE.; Brambilla, P.; Sassi, RB.; Mallinger, AG.; Soares, JC. Lithium Effects on Human Brain Structure Mapped Using Longitudinal MRI. Washington, DC: Society for Neuroscience; 2005b.

Leporé N, Brun C, Chou YY, Chiang MC, Dutton RA, Hayashi KM, Luders E, Lopez OL, Aizenstein HJ, Toga AW, Becker JT, Thompson PM. Generalized tensor-based morphometry of HIV/AIDS using multivariate statistics on deformation tensors. IEEE Trans Med Imaging. 2008; 27:129–141. [PubMed: 18270068]

Leporé N, Brun C, Chou YY, Lee AD, Barysheva M, Pennec X, McMahon KL, Meredith M, de Zubicaray G, Wright MJ, Toga AW, Thompson PM. Best Individual Template Selection from Deformation Tensor Minimization. ISBI. 2008; 2008 in press, Feb. 2008.

Leporé, N.; Brun, C.; Pennec, X.; Chou, Y.; Lopez, O.; Aizenstein, H.; Becker, J.; Toga, A.; Thompson, P. Mean Template for Tensor-Based Morphometry using Deformation Tensors. Brisbane, Australia: MICCAI; 2007.

Lorenzen P, Prastawa M, Davis B, Gerig G, Bullitt E, Joshi S. Multi-modal image set registration and atlas formation. Med Image Anal. 2006; 10:440–451. [PubMed: 15919231]

Marsden, J.; Hughes, T. Mathematical foundations of elasticity. Prentice-Hall; 1983.

Martins CA, Oulhaj A, de Jager CA, Williams JH. APOE alleles predict the rate of cognitive decline in Alzheimer disease: a nonlinear model. Neurology. 2005; 65:1888–1893. [PubMed: 16380608]

Mazziotta J, Toga A, Evans A, Fox P, Lancaster J, Zilles K, Woods R, Paus T, Simpson G, Pike B, Holmes C, Collins L, Thompson P, MacDonald D, Iacoboni M, Schormann T, Amunts K, Palomero-Gallagher N, Geyer S, Parsons L, Narr K, Kabani N, Le Goualher G, Boomsma D, Cannon T, Kawashima R, Mazoyer B. A probabilistic atlas and reference system for the human brain: International Consortium for Brain Mapping (ICBM). Philos Trans R Soc Lond B Biol Sci. 2001; 356:1293–1322. [PubMed: 11545704]

McKhann G, Drachman D, Folstein M, Katzman R, Price D, Stadlan EM. Clinical diagnosis of Alzheimer's disease: report of the NINCDS-ADRDA Work Group under the auspices of Department of Health and Human Services Task Force on Alzheimer's Disease. Neurology. 1984; 34:939–944. [PubMed: 6610841]

Moffat SD, Szekely CA, Zonderman AB, Kabani NJ, Resnick SM. Longitudinal change in hippocampal volume as a function of apolipoprotein E genotype. Neurology. 2000; 55:134–136. [PubMed: 10891924]

Morris JC. The Clinical Dementia Rating (CDR): current version and scoring rules. Neurology. 1993; 43:2412–2414. [PubMed: 8232972]

Mueller SG, Weiner MW, Thal LJ, Petersen RC, Jack C, Jagust W, Trojanowski JQ, Toga AW, Beckett L. The Alzheimer's disease neuroimaging initiative. Neuroimaging Clin N Am. 2005a; 15:869–877. xi–xii. [PubMed: 16443497]

Mueller SG, Weiner MW, Thal LJ, Petersen RC, Jack CR, Jagust W, Trojanowski JQ, Toga AW, Beckett L. Ways toward an early diagnosis in Alzheimer's disease: The Alzheimer's Disease Neuroimaging Initiative (ADNI). Alzheimers Dement. 2005b; 1:55–66. [PubMed: 17476317]

Nichols TE, Holmes AP. Nonparametric permutation tests for functional neuroimaging: a primer with examples. Hum Brain Mapp. 2002; 15:1–25. [PubMed: 11747097]

Petersen RC. Aging, mild cognitive impairment, and Alzheimer's disease. Neurol Clin. 2000; 18:789–806. [PubMed: 11072261]

Petersen RC, Doody R, Kurz A, Mohs RC, Morris JC, Rabins PV, Ritchie K, Rossor M, Thal L, Winblad B. Current concepts in mild cognitive impairment. Arch Neurol. 2001; 58:1985–1992. [PubMed: 11735772]

Petersen RC, Smith GE, Waring SC, Ivnik RJ, Tangalos EG, Kokmen E. Mild cognitive impairment: clinical characterization and outcome. Arch Neurol. 1999; 56:303–308. [PubMed: 10190820]

Price JL, Morris JC. Tangles and plaques in nondemented aging and "preclinical" Alzheimer's disease. Ann Neurol. 1999; 45:358–368. [PubMed: 10072051]

Riddle WR, Li R, Fitzpatrick JM, DonLevy SC, Dawant BM, Price RR. Characterizing changes in MR images with color-coded Jacobians. Magn Reson Imaging. 2004; 22:769–777. [PubMed: 15234445]

Ridha BH, Anderson VM, Barnes J, Boyes RG, Price SL, Rossor MN, Whitwell JL, Jenkins L, Black RS, Grundman M, Fox NC. Volumetric MRI and cognitive measures in Alzheimer disease : Comparison of markers of progression. J Neurol. 2008

Roses AD, Saunders AM. APOE is a major susceptibility gene for Alzheimer's disease. Curr Opin Biotechnol. 1994; 5:663–667. [PubMed: 7765750]

Saunders AM, Strittmatter WJ, Schmechel D, George-Hyslop PH, Pericak-Vance MA, Joo SH, Rosi BL, Gusella JF, Crapper-MacLachlan DR, Alberts MJ, et al. Association of apolipoprotein E allele epsilon 4 with late-onset familial and sporadic Alzheimer's disease. Neurology. 1993; 43:1467–1472. [PubMed: 8350998]

Scahill RI, Frost C, Jenkins R, Whitwell JL, Rossor MN, Fox NC. A longitudinal study of brain volume changes in normal aging using serial registered magnetic resonance imaging. Arch Neurol. 2003; 60:989–994. [PubMed: 12873856]

Shattuck DW, Leahy RM. BrainSuite: an automated cortical surface identification tool. Med Image Anal. 2002; 6:129–142. [PubMed: 12045000]

Silbert LC, Quinn JF, Moore MM, Corbridge E, Ball MJ, Murdoch G, Sexton G, Kaye JA. Changes in premorbid brain volume predict Alzheimer's disease pathology. Neurology. 2003; 61:487–492. [PubMed: 12939422]

Sled JG, Zijdenbos AP, Evans AC. A nonparametric method for automatic correction of intensity nonuniformity in MRI data. IEEE Trans Med Imaging. 1998; 17:87–97. [PubMed: 9617910]

Smith CD, Chebrolu H, Wekstein DR, Schmitt FA, Jicha GA, Cooper G, Markesbery WR. Brain structural alterations before mild cognitive impairment. Neurology. 2007; 68:1268–1273. [PubMed: 17438217]

Sowell ER, Peterson BS, Kan E, Woods RP, Yoshii J, Bansal R, Xu D, Zhu H, Thompson PM, Toga AW. Sex differences in cortical thickness mapped in 176 healthy individuals between 7 and 87 years of age. Cereb Cortex. 2007; 17:1550–1560. [PubMed: 16945978]

Sowell ER, Peterson BS, Thompson PM, Welcome SE, Henkenius AL, Toga AW. Mapping cortical change across the human life span. Nat Neurosci. 2003; 6:309–315. [PubMed: 12548289]

Studholme C, Cardenas V. A template free approach to volumetric spatial normalization of brain anatomy. Pattern Recognition Letters. 2004; 25:1191–1202.

Thompson P, Apostolova L. Computational Anatomical Methods as Applied to Aging and Dementia. British Journal of Radiology. 2007 in press, Feb. 14, 2008 [Invited Article].

Thompson PM, Giedd JN, Woods RP, MacDonald D, Evans AC, Toga AW. Growth patterns in the developing brain detected by using continuum mechanical tensor maps. Nature. 2000a; 404:190–193. [PubMed: 10724172]

Thompson PM, Hayashi KM, de Zubicaray G, Janke AL, Rose SE, Semple J, Herman D, Hong MS, Dittmer SS, Doddrell DM, Toga AW. Dynamics of gray matter loss in Alzheimer's disease. J Neurosci. 2003; 23:994–1005. [PubMed: 12574429]

Thompson PM, Woods RP, Mega MS, Toga AW. Mathematical/computational challenges in creating deformable and probabilistic atlases of the human brain. Hum Brain Mapp. 2000b; 9:81–92. [PubMed: 10680765]

Toga, AW. Brain Warping. 1st ed. San Diego: Academic Press; 1999.

Tohgi H, Takahashi S, Kato E, Homma A, Niina R, Sasaki K, Yonezawa H, Sasaki M. Reduced size of right hippocampus in 39- to 80-year-old normal subjects carrying the apolipoprotein E epsilon4 allele. Neurosci Lett. 1997; 236:21–24. [PubMed: 9404942]

Wechsler, D. WMS-R Wechsler Memory Scale - Revised Manual. New York: The Psychological Corporation, Harcourt Brace Jovanovich, Inc.; 1987.

Wishart HA, Saykin AJ, McAllister TW, Rabin LA, McDonald BC, Flashman LA, Roth RM, Mamourian AC, Tsongalis GJ, Rhodes CH. Regional brain atrophy in cognitively intact adults with a single APOE epsilon4 allele. Neurology. 2006; 67:1221–1224. [PubMed: 17030756]

Zannis VI, Breslow JL. Apolipoprotein E. Mol Cell Biochem. 1982; 42:3–20. [PubMed: 7038438]

Zannis VI, Breslow JL, Utermann G, Mahley RW, Weisgraber KH, Havel RJ, Goldstein JL, Brown MS, Schonfeld G, Hazzard WR, Blum C. Proposed nomenclature of apoE isoproteins, apoE genotypes, and phenotypes. J Lipid Res. 1982; 23:911–914. [PubMed: 7130859]
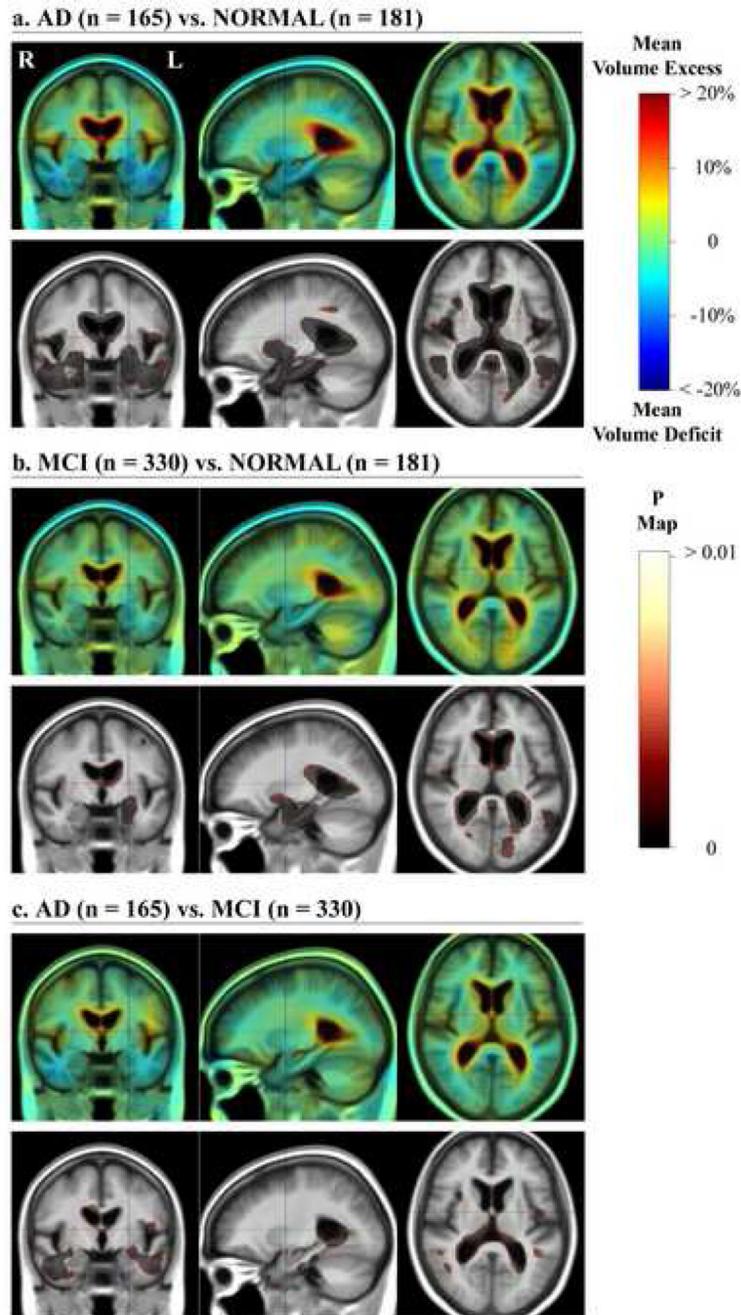
Figure 1. 3D Maps of Brain Atrophy
The top rows of panels a, b, and c show the mean level of atrophy as a percentage reduction in volume. The bottom rows show the significance of these reductions, revealing highly significant atrophy in AD but a more anatomically restricted atrophic pattern in MCI. In MCI (b), atrophy is most prominent in the left hippocampus; as expected (Carmichael et al., 2007a, b), ventricular expansion is also substantial. When MCI is compared with AD (c), additional temporal lobe degeneration is evident. The overall level of ventricular expansion is about 10–15% for MCI and greater than 20% for the AD group.
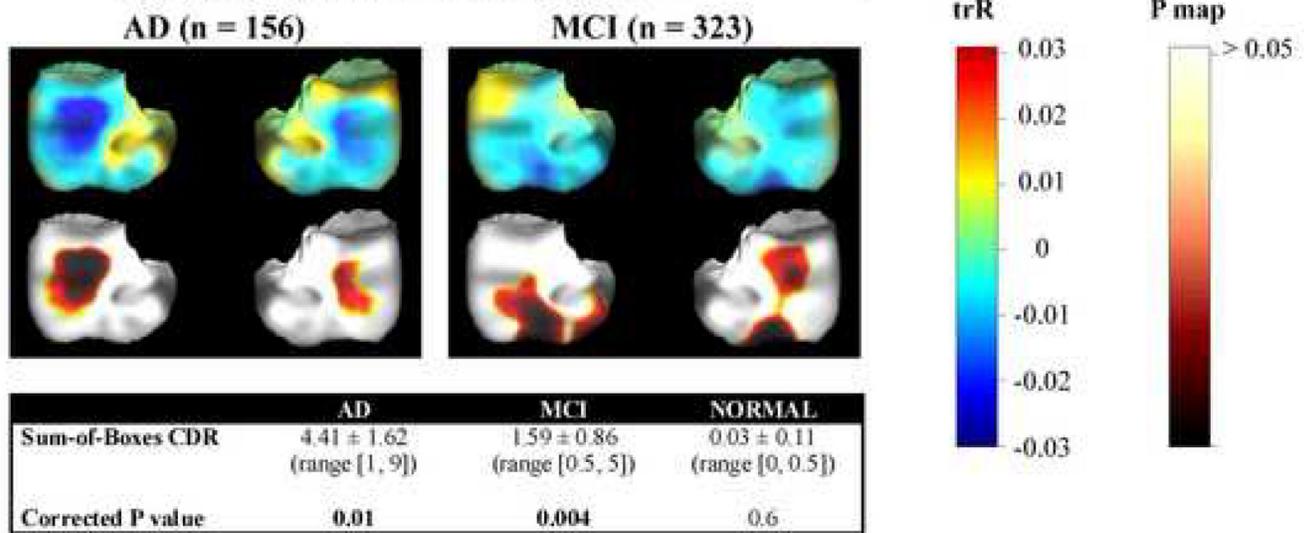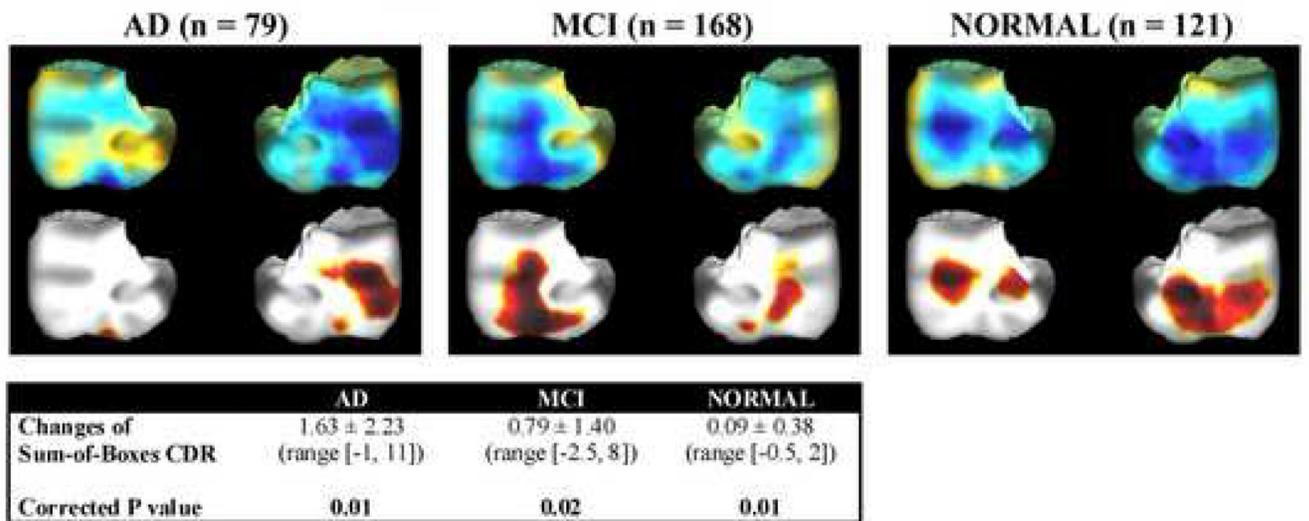
Figure 2. Temporal Lobe Atrophy Correlates with Sum-of-Boxes Clinical Dementia Rating and Future Clinical Decline

(a) Negative correlations are detected between temporal lobe atrophy and higher CDR scores at the time of the initial scan. The corrected P values in the table (inset) provide an overall estimate of significance, corrected for multiple comparisons. (b) Atrophy of the temporal lobe also predicts future cognitive decline, as reflected by an increase in CDR scores, which indicates deteriorating cognitive function over the following year. trR denotes partial correlation coefficient.

Regression with MMSE and Changes of MMSE

a. MMSE in MCI (n = 330)
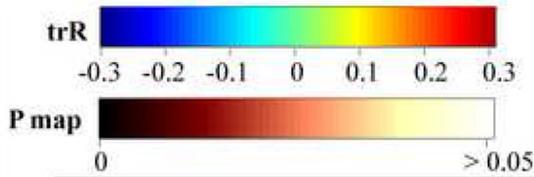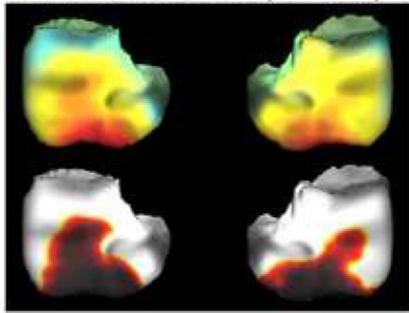
	AD	MCI	NORMAL
MMSE	23.27 ± 2.03 (range [18, 27])	27.03 ± 1.81 (range [23, 30])	29.13 ± 0.97 (range [25, 30])
Corrected P value	0.1	**<0.001**	0.2

b. Changes of MMSE in AD (n = 74)
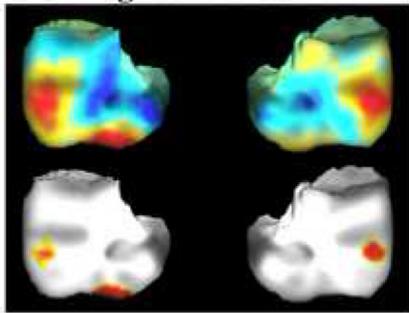
	AD	MCI	NORMAL
Changes of MMSE	-2.27 ± 4.29 (range [-18, 5])	-0.99 ± 2.75 (range [-12, 4])	-0.07 ± 1.37 (range [-5, 3])
Corrected P value	**0.01**	0.4	0.7

Figure 3. Temporal Lobe Atrophy Correlates with Mini-Mental State Examination and Future Clinical Decline

(a) In MCI, positive correlations are detected between temporal lobe atrophy and lower MMSE scores at the time of the initial scan. (b) In the AD group, atrophy in the temporal lobe also predicts future cognitive decline, as reflected by a decrease in MMSE scores over the following year, which indicates deteriorating cognitive function over time. trR denotes partial correlation coefficient.

4a. Regression with Logical Memory Test (immediate)

AD (n = 156)   MCI (n = 323)   NORMAL (n = 179)
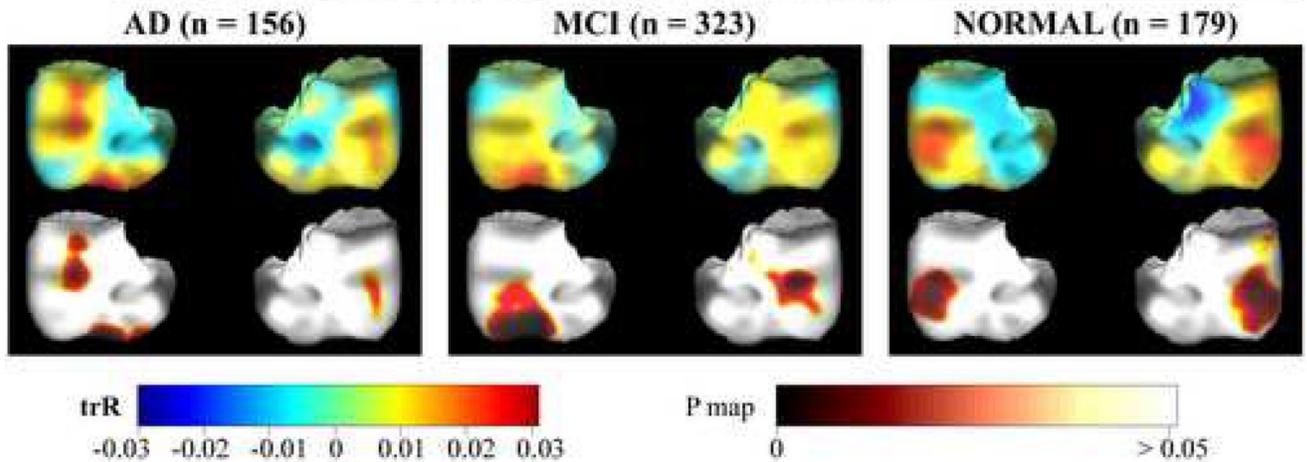
	AD	MCI	NORMAL
Logical Memory Test (immediate)	3.99 ± 2.95 (range [0, 13])	7.17 ± 3.25 (range [0, 18])	13.92 ± 3.39 (range [5, 21])
Corrected P value	0.03	0.02	0.008

4b. Regression with Logical Memory Test (delay)

AD (n = 156)   MCI (n = 323)   NORMAL (n = 179)
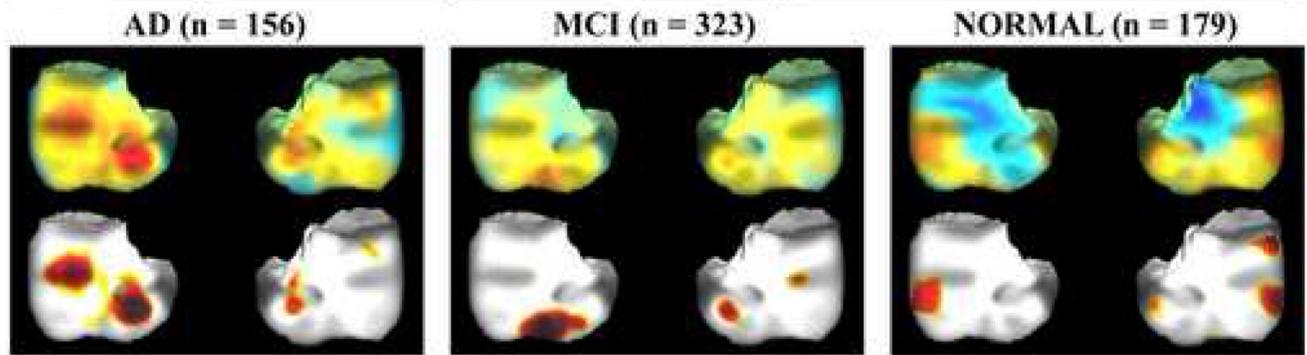
	AD	MCI	NORMAL
Logical Memory Test (delay)	1.24 ± 1.83 (range [0, 8])	3.86 ± 2.76 (range [0, 12])	13.01 ± 3.59 (range [5, 22])
Corrected P value	0.01	0.03	0.008

Figure 4. Temporal Lobe Atrophy correlates with scores on the WMS-R Logical Memory Test, for both Immediate and Delayed Conditions
Positive correlations are detected between baseline temporal lobe atrophy and lower logical memory test scores for both immediate (a) and delayed (b) conditions, in temporal lobe regions. trR denotes partial correlation coefficient.

Association between Jacobian values and conversion to AD

MCI (n = 186)
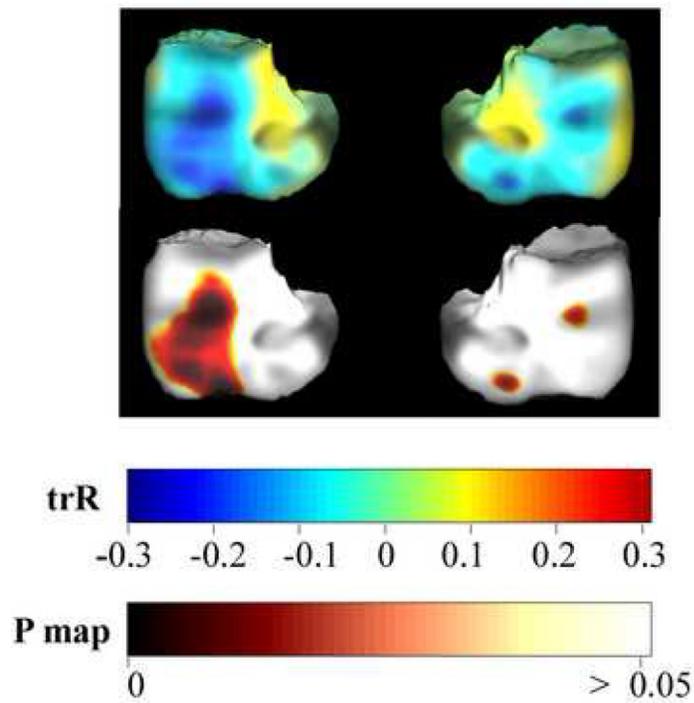
Figure 5. Association between temporal lobe atrophy and conversion to AD during the one-year period after the scan
Subjects who converted from MCI to AD over a period of one year after their first scan were coded as "1"; nonconverters were coded as "0". A negative correlation suggests that temporal lobe degeneration predicts future conversion to AD.

Figure 6. Effects of ApoE

a. NORMAL: ApoE3/3 vs. 2/2 + 2/3
(n= 52, neg P = 0.03, ROI: CSF)

-30% -20% -10% 0 10% 20% 30%

c. MCI: 3/4 vs. 4/4
(n=68, neg P=0.001, ROI: Hippocampi)

-10%   -5%   0   5%   10%

b. MCI: ApoE3/3 vs. 3/4
(n=68, pos P=0.019, ROI: CSF)

-20%   -10%   0   10%   20%

d. AD: 3/4 vs. 4/4
(n=64, neg P=0.01, ROI: Hippocampi;
neg P = 0.02, ROI: Temporal Lobes)

-10%   -5%   0   5%   10%
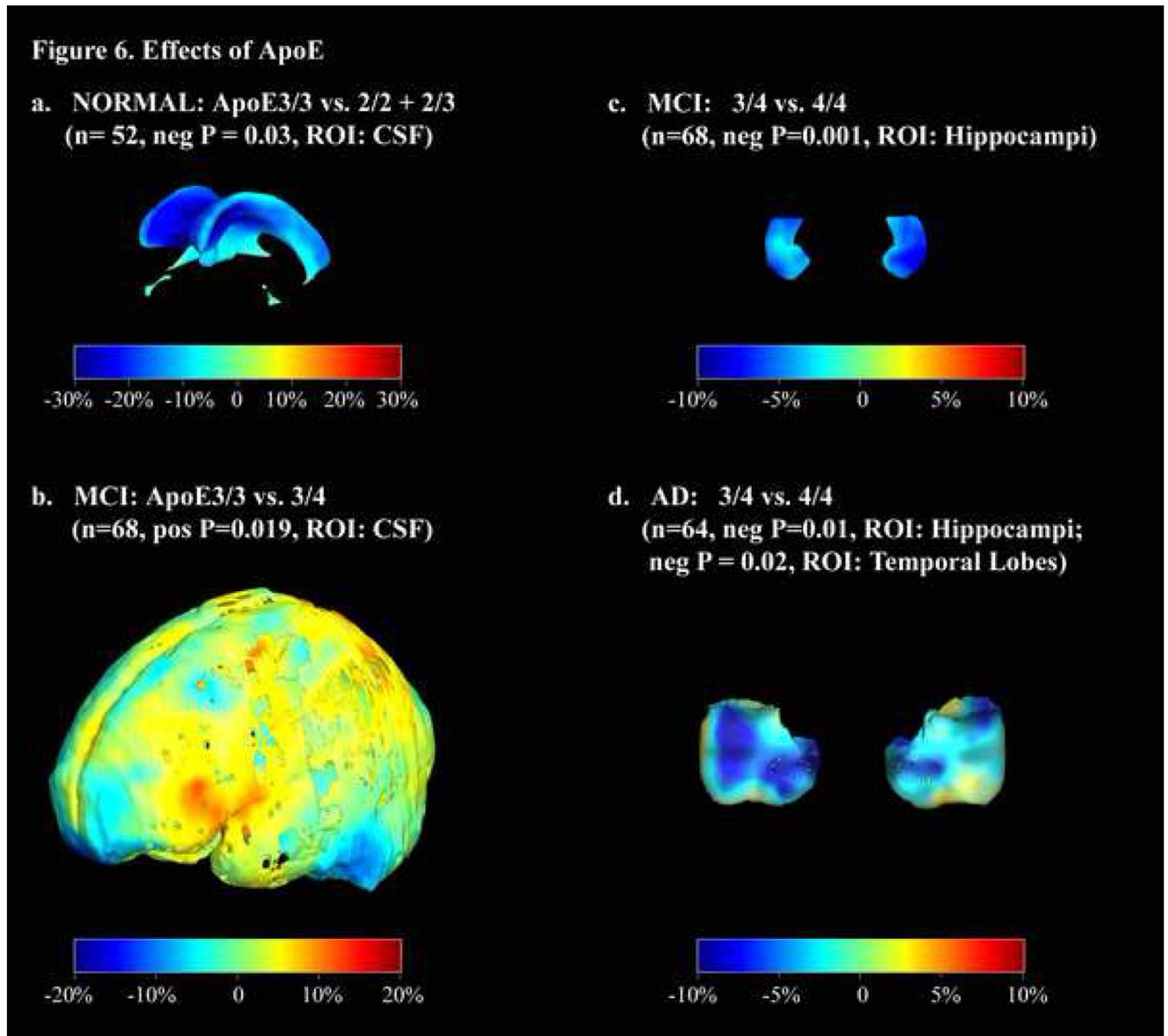
Figure 6. ApoE gene effects
Maps show the mean percent differences in regional brain volumes for four different group comparisons. Percent differences are displayed on models of the regions implicated: (a) ventricular CSF, (b) sulcal CSF, (c) hippocampi, and (d) temporal lobes; dotted lines show the boundary of the hippocampus.

Table 1

Demographic and cognitive data for the subjects included in this study.

	AGE (mean ± SD)	CDR-SB	MMSE	Logical Memory Test	
				Immediate	Delay
AD	75.6 ± 7.6	4.41 ± 1.62	23.27 ± 2.03	3.99 ± 2.95	1.24 ± 1.83
MCI	74.8 ± 7.5	1.59 ± 0.86	27.03 ± 1.81	7.17 ± 3.25	3.86 ± 2.76
NORMAL	75.9 ± 5.1	0.03 ± 0.11	29.13 ± 0.97	13.92 ± 3.39	13.01 ± 3.59

Table 2

Frequency of ApoE genotypes in the AD, MCI and NORMAL groups

AD (n = 156; 83 males +73 females)

	Men		Women		All	
	N	%	N	%	N	%
ε2/ε2	0	0.0	0	0.0	0	0.0
ε2/ε3	1	1.2	2	2.7	3	1.9
ε2/ε4	0	0.0	4	5.5	4	2.6
ε3/ε3	23	27.7	26	35.6	49	31.4
ε3/ε4	42	50.6	27	37.0	69	44.2
ε4/ε4	17	20.5	14	19.2	31	19.9

MCI (n = 323; 204 males +119 females)

	Men		Women		All	
	N	%	N	%	N	%
ε2/ε2	0	0.0	0	0.0	0	0.0
ε2/ε3	7	3.4	8	6.7	15	4.6
ε2/ε4	5	2.5	2	1.7	7	2.2
ε3/ε3	97	47.5	43	36.1	140	43.3
ε3/ε4	77	37.7	49	41.2	126	39.0
ε4/ε4	18	8.8	16	13.4	34	10.5

NORMAL (n = 179; 89 males +90 females)

	Men		Women		All	
	N	%	N	%	N	%
ε2/ε2	2	2.2	0	0.0	2	1.1
ε2/ε3	9	10.1	17	18.9	26	14.5
ε2/ε4	2	2.2	1	1.1	3	1.7
ε3/ε3	58	65.2	49	54.4	107	59.8
ε3/ε4	17	19.1	21	23.3	38	21.2
ε4/ε4	3	3.4	2	2.2	5	2.8